

A glial origin for periventricular nodular heterotopia caused by impaired expression of Filamin-A

Aurelie Carabalona^{1,2,3}, Shirley Beguin^{1,2,3}, Emilie Pallesi-Pocachard^{1,2,3}, Emmanuelle Buhler^{3,4}, Christophe Pellegrino^{1,2,3}, Karen Arnaud^{1,2,3}, Philippe Hubert⁵, Mehdi Oualha⁵, Jean Pierre Siffroi⁶, Sabrina Khantane^{1,2,3}, Isabelle Coupry⁷, Cyril Goizet⁷, Antoinette Bernabe Gelot⁸, Alfonso Represa^{1,2,3} and Carlos Cardoso^{1,2,3,*}

¹INMED, Parc Scientifique de Luminy, Marseille, France, ²Université de la Méditerranée, UMR S901 Aix-Marseille 2, Marseille, France, ³Inserm Unité 901, Marseille, France, ⁴Plateforme postgénomique INMED-INSERM, Parc Scientifique de Luminy, Marseille, France, ⁵Service de Réanimation Pédiatrique et de Néonatalogie, Hôpital Necker Enfants Malades, Paris, France, ⁶Service de Génétique et d'Embryologie Médicales, Hôpital A. Trousseau, Paris, France, ⁷Laboratoire Maladies Rares: Génétique et Métabolisme (MRGM), Université Bordeaux, EA4576 Bordeaux, France and ⁸Département de Neuropathologie, Service d'Anatomie et Cytologie Pathologiques, Hôpital A. Trousseau, Paris, France

Received August 23, 2011; Revised and Accepted November 7, 2011

Periventricular nodular heterotopia (PH) is a human brain malformation caused by defective neuronal migration that results in ectopic neuronal nodules lining the lateral ventricles beneath a normal appearing cortex. Most affected patients have seizures and their cognitive level varies from normal to severely impaired. Mutations in the *Filamin-A* (or *FLNA*) gene are the main cause of PH, but the underlying pathological mechanism remains unknown. Although two *FlnA* knockout mouse strains have been generated, none of them showed the presence of ectopic nodules. To recapitulate the loss of *FlnA* function in the developing rat brain, we used an *in utero* RNA interference-mediated knockdown approach and successfully reproduced a PH phenotype in rats comparable with that observed in human patients. In *FlnA*-knockdown rats, we report that PH results from a disruption of the polarized radial glial scaffold in the ventricular zone altering progression of neural progenitors through the cell cycle and impairing migration of neurons into the cortical plate. Similar alterations of radial glia are observed in human PH brains of a 35-week fetus and a 3-month-old child, harboring distinct *FLNA* mutations not previously reported. Finally, juvenile *FlnA*-knockdown rats are highly susceptible to seizures, confirming the reliability of this novel animal model of PH. Our findings suggest that the disorganization of radial glia is the leading cause of PH pathogenesis associated with *FLNA* mutations.

***Rattus norvegicus FlnA* mRNA (GenBank accession number FJ416060).**

INTRODUCTION

Congenital malformations of the cerebral cortex are important causes of mental retardation and account for 20–40% of drug-resistant epilepsy in childhood (1). Among these cortical malformations, periventricular nodular heterotopia (PH) represents a clinically and genetically heterogeneous group of neuronal migration disorders. PH is characterized by nodules of neurons ectopically placed along the walls of the lateral

ventricles (2,3). PH, often bilateral, occurred predominantly in women as an X-linked dominant trait associated with high rates of prenatal hemizygous male lethality (2,4,5). Mutations in the *Filamin-A* (or *FLNA*) gene, on Xq28, were found in 100% of families with X-linked bilateral PH and in 26% of sporadic patients with PH (4,6). The low percentage of *FLNA* mutations in sporadic cases could be explained by low somatic mosaicism (7), as well as the viability of some affected males (5,8). Heterozygous women present seizures

*To whom correspondence should be addressed at: INMED, INSERM U901, Parc Scientifique de Luminy, BP13, 13009 Marseille, France. Tel: +33 491828130; Fax: +33 491828101; Email: cardoso@inmed.univ-mrs.fr

that are difficult to control and normal to borderline intelligence (4,5). *FLNA* is widely expressed in brain as well as in many other tissues and encodes a large (280 kDa) cytoplasmic actin-binding phosphoprotein (9). Dimerization of *FLNA* protein allows the formation of a V-shaped flexible structure which crosslinks actin filaments into orthogonal networks (10). It also regulates reorganization of the actin cytoskeleton by interacting with several proteins at the plasma membrane, leading to changes in cell shape and migration (11). Accordingly, an *FLNA*-deficient human melanoma cell line shows motility defects (12), suggesting that PH in humans likely results from the disruption of neuronal migration during cortical development. The high prevalence of *FLNA* mutations resulting in truncations of the actin-binding domain (6) indicates that *FLNA*'s ability to crosslink actin may be essential for neuronal migration. Thus, expression of *FlnA* lacking the actin-binding domain in the mouse neocortex leads to neuronal migration arrest in the subventricular (SVZ) and intermediate zones (IZ) (13). However, *FlnA* knockout mice, which die during midgestation (14,15), did not develop PH or presence of misplaced neurons in the neocortical VZ/IZ (14). Interestingly, the complete loss of mitogen-activated protein kinase kinase 4 (MEKK4), a regulator of *FlnA* protein phosphorylation, produces PH in mice (16). These data suggest that alternate pathways or possible gene interactions may account for the fact that *FlnA* knockout mice generated so far do not exhibit PH (14,15). Thus, development of a more appropriate *FlnA* animal model could improve our understanding of mechanisms underlying the genesis of PH.

To address this limitation, we used an *in utero* RNA interference (RNAi)-mediated knockdown approach (17) to recapitulate the loss of function of *FlnA* in the developing rat brain. This method has proved very powerful to develop animal models of brain disorders involving similar proteins and mechanisms to that observed in human patients (18,19). Moreover, *in vivo* RNAi allows fast and spatio-temporal modulation of gene expression that presents considerable advantages compared with classical genetically modified rodent models. Here, we show that *in utero* knockdown of *FlnA* expression in neural progenitors impairs their cell-cycle progression as well as their migration by disrupting the organization of radial glia and leads to a PH phenotype in the rat neocortex. Consistent with the observations made in rodents, similar alterations in radial glial organization are observed around periventricular nodules in postmortem brains of two female patients carrying distinct *FLNA* mutations (Q231X and R2103QfsX56, respectively). Finally, we validate our new animal model of PH by showing that juvenile *FlnA*-knockdown rats display a higher susceptibility to pentylenetetrazole (PTZ)-induced seizures. Overall, our data highlight the critical role of *FLNA* in radial glia organization and function for neurogenesis and migration and also provide insight into the molecular pathogenesis of human PH.

RESULTS

Expression of *FlnA* in the developing rat brain

To assess how *FlnA* contributes to cortical development, we examined the spatial and temporal expression patterns of

FlnA in the rat neocortex. Western blot analysis of whole-brain protein extracts, from embryonic day 13 (E13) to postnatal day 30 (P30) rats, showed that *FlnA* was expressed at all embryonic stages but markedly reduced after P11 (Fig. 1A). Moreover, immunohistochemical stainings revealed strong labeling of *FlnA* in the VZ/IZ of the rat neocortex at E14, when neuronal migration is underway (Fig. 1B and C). By E20, when neuronal migration is largely completed, expression of *FlnA* was restricted to the ventricular zone (Fig. 1D and E) and persisted in the periventricular region until P7 (Fig. 1F and G). Altogether, these findings suggested that *FlnA* is specifically expressed in the VZ at embryonic stages, and decreases during postnatal development. Moreover, our data are consistent with previous studies showing the expression of *FlnA* in the developing mouse neocortex (9). The VZ of the developing rat neocortex is composed predominantly of radial glial cells and neural precursors (20). Double-immunohistochemical studies showed that in tissue sections of E17 rat neocortex, radial glial cells that express vimentin co-expressed *FlnA* in the VZ/IZ (Fig. 1H–J). Furthermore, nestin, which is also expressed by radial glia cells, co-localized with *FlnA* (Fig. 1K–M). Our results also demonstrated a strong colocalization of PSA-NCAM, a marker of immature neurons, and *FlnA* stainings along the ventricular border (Fig. 1N). However, most PSA-NCAM-positive immature neurons in the VZ/IZ were faintly stained for *FlnA* (Fig. 1N–P). Interestingly, no colocalization between the early pan-neuronal marker class III β -tubulin (TuJ1) and *FlnA* was observed in E17 and E20 rat neocortex (data not shown). Altogether, these data suggest that *FlnA* is predominantly expressed by radial glial cells and neuronal progenitors cells.

In utero RNAi of *FlnA* impairs radial migration

To further explore the function of *FlnA* in corticogenesis, we used the *in utero* RNAi approach to knockdown *FlnA* expression in rat embryonic neuronal progenitor cells. For this purpose, we generated two small-hairpin RNAs (shRNAs) targeting either the coding sequence (CDS_{hp}) or the 3'-untranslated region (3'UTR_{hp}) of the rat *FlnA* mRNA (Fig. 2A) and the two corresponding ineffective shRNAs with three point mutations creating mismatches, CDS_{m3hp} and 3'UTR_{m3hp}. These shRNAs were transiently transfected into rat C6 glioma cells to evaluate their capacity to repress endogenous *FlnA* expression. We found that CDS_{hp} and 3'UTR_{hp}, but not the two ineffective shRNAs, significantly decreased *FlnA* mRNA levels by 60–70%, resulting in a notable reduction in *FlnA* protein as assessed by western blot analysis (Fig. 2B and C). To determine whether knockdown of *FlnA* expression alters neuronal migration, either 3'UTR_{hp} or 3'UTR_{m3hp} combined with a red fluorescent protein (RFP) construct was introduced into neural progenitor cells of rat neocortex by *in utero* electroporation at E15. This time of development corresponds to the period of migration of layers II/III neurons and the highest levels of *FlnA* expression in the cortex (Fig. 1A). The distribution of RFP-positive cells was analyzed 2 and 5 days later (Fig. 2D and F). At E17, cells transfected with the RFP construct alone ($78.5 \pm 4.7\%$; $n = 11$ embryos) or combined with 3'UTR_{hp} ($87.4 \pm 3.6\%$; $n =$

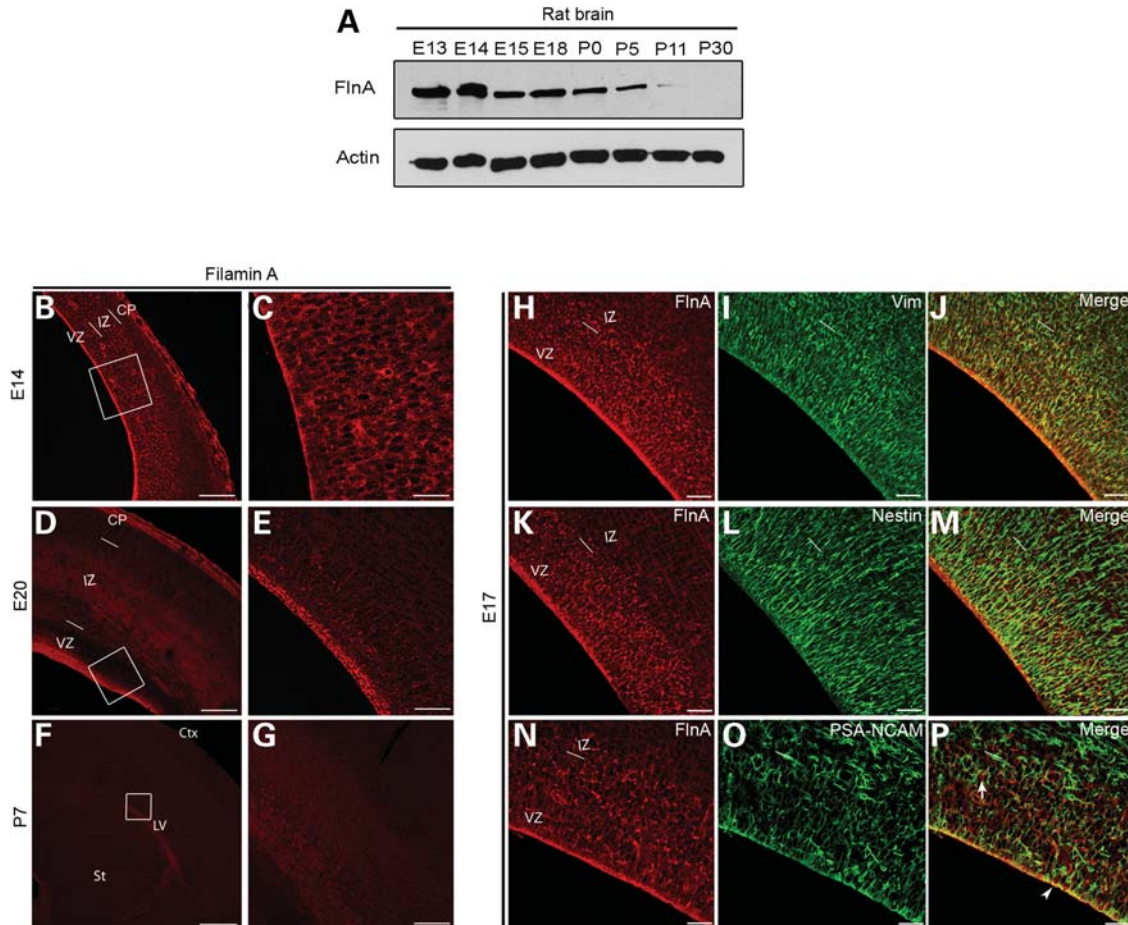


Figure 1. FlnA is expressed by radial glia and neural progenitors at the ventricular surface of the developing rat cortex. (A) Western blot analysis of rat FlnA protein levels during brain development at the indicated time points (top). FlnA was expressed during embryonic stages but markedly reduced after P11. Brain homogenates were immunoblotted for actin as a loading control (bottom). (B–G) Immunohistochemistry revealed strong labeling of FlnA in the VZ/IZ of E14 brain coronal section (B), restricted to the VZ at E20 (D) and persisted in the periventricular zone until P7 (F). (C, E and G) Higher magnification images of areas outlined in (B), (D) and (F). (H–J) Higher magnification confocal images of cortical sections at E17 showing overlay (J) of FlnA (H, red), and vimentin (I, green) to label radial fibers in the VZ/IZ. (K–M) Double-immunostaining for FlnA (H, red), nestin (I, green) and the merger of the two (J) showing that both proteins are associated with VZ radial glial cells. (N–P) Immunohistological analysis with FlnA (N, red) and immature neuronal marker PSA-NCAM (O, green) showing a strong colocalization along the ventricular border (P, arrowhead). However, most PSA-NCAM-positive cells in the VZ/IZ faintly express FlnA (arrow in P). Scale bars: 500 μ m (F); 200 μ m (D); 100 μ m (B, C, E, G and H–M).

9 embryos) or 3UTRm3hp (73.8 \pm 5.2%; n = 8 embryos) were largely found in the VZ/IZ (Fig. 2D and E). However, in the upper IZ of 3UTRhp transfected brains (n = 10), we found a significantly higher percentage of non-radially oriented RFP-positive cells with a bipolar morphology compared with control brains transfected with RFP alone (n = 10) or together with 3UTRm3hp (n = 10) (Supplementary Material, Fig. S1). By E20, the majority of RFP (90.1 \pm 2.14%; n = 10 embryos) or 3UTRm3hp (81.4 \pm 2.3%; n = 9 embryos) transfected cells reached the cortical plate (Fig. 2F and G). In contrast, the expression of 3UTRhp led to a significant arrest of transfected cells in the VZ/IZ, with only 32.4 \pm 3.9% (n = 12 embryos; P < 0.001) of RFP-positive cells reaching the cortical plate (Fig. 2F and G). To rule out the possibility that this phenotype was due to off-target effects of 3UTRhp, we first conducted similar experiments with CDSHp construct (n = 4 embryos) and the same migration defect was observed (Supplementary Material,

Fig. S2). We next performed a rescue experiment in which we co-transfected the 3UTRhp along with an FlnA-IRES-GFP construct driving the expression of the full-length rat FlnA coding sequence and GFP as a reporter (Supplementary Material, Fig. S3). Previous studies have shown that overexpression of full-length human FLNA in E14.5 mouse neocortex slightly delays radial migration in the upper cortical plate at E18 (16). However, in our experimental conditions, we observed in E20 rat brains (n = 9 embryos) that neurons electroporated 5 days previously with our FlnA-IRES-GFP construct alone reached the cortical plate as expected (Fig. 3A–C). Combined expression of FlnA-IRES-GFP with 3UTRhp prevented migration arrest of transfected cells in the VZ at E20, demonstrating the target specificity of the shRNA effect (Fig. 3D–F). Nevertheless, partial rescue of the FlnA knockdown phenotype was observed in the IZ (Fig. 3E), which could result from dilution of the FlnA-IRES-GFP construct due to cell division. Altogether, these results support an

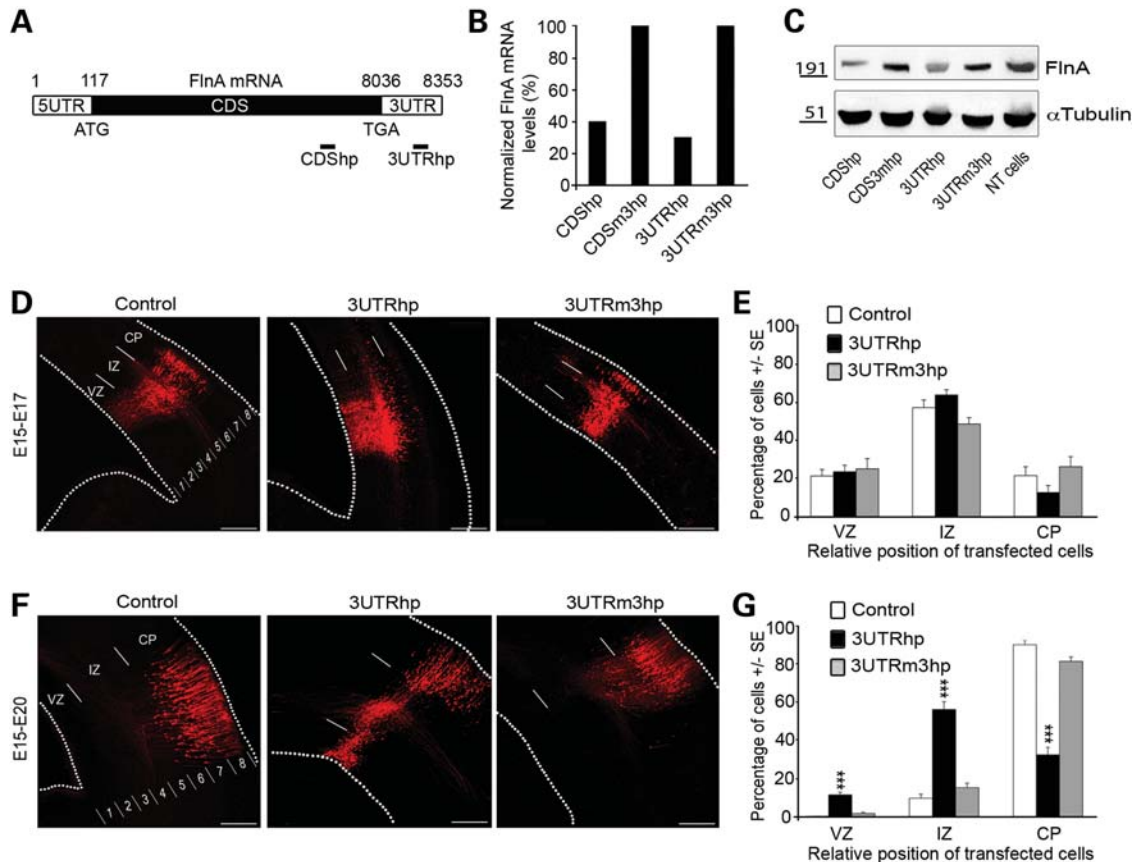


Figure 2. *In utero* knockdown of FlnA expression by RNAi alters neuronal migration in embryonic rat neocortex. (A) Schematic diagram showing the position of small-hairpin RNAs targeting the coding sequence (CDSshp) and the 3'UTR (3UTRshp) of FlnA mRNA. (B) Knockdown of endogenous FlnA mRNA expression in rat C6 glioma cells was measured by qPCR 48 h after transfection with CDSshp or 3UTRshp. We observed a reduction of FlnA mRNA expression ranging from 60–70% compared with corresponding ineffective shRNAs (CDSsm3hp and 3UTRm3hp). Cyclophilin A was used for normalization. (C) Western blot analysis revealed that FlnA protein levels, 48 h after transfection, were much lower in cells transfected with CDSshp or 3UTRshp compared with those transfected with CDSsm3hp or 3UTRm3hp and with non-transfected (NT) cells. α -Tubulin was used for normalization. (D and F) Representative neocortical coronal sections showing migration of transfected cells 2 (D) and 5 days (F) after electroporation at E15 with either RFP construct alone (control) or combined with 3UTRshp or 3UTRm3hp. (E and G) Quantification (means \pm SEM) of RFP-positive cell distribution in eight arbitrary strata dividing the cortex. RFP-positive cells were counted in strata 1 and 2 corresponding to the ventricular zone (VZ), in strata 3, 4 and 5 to the intermediate zone (IZ) and strata 6, 7 and 8 to the cortical plate (CP) and expressed as a percentage of the total. Quantification of independent brains was carried out after 2 days (E) (RFP, $n = 11$; 3UTRshp, $n = 9$; 3UTRm3hp, $n = 8$) or 5 days (G) (RFP, $n = 10$; 3UTRshp, $n = 12$; 3UTRm3hp, $n = 9$) after transfection at E15. $***P < 0.001$ when compared with control and 3UTRm3hp (E and G). Scale bars: 200 μ m.

involvement of FlnA in radial neuronal migration during cortical development.

FlnA-knockdown rats exhibit PH

In order to evaluate whether this impaired neuronal migration leads to PH formation, we examined postnatal brains following embryonic knockdown of FlnA expression. We found ectopic nodules of RFP-positive cells lining the ventricular wall in all 3UTRshp transfected brains examined at P7 ($n = 13$; Fig. 4B) or at P30 ($n = 9$; data not shown) compared with controls ($n = 15$; Fig. 4A). In all P7 FlnA-knockdown pups, the average nodule size ranged from 0.17 to 0.37 mm². They contained a mixture of RFP-transfected and -non-transfected cells, which were positive for the mature neuronal markers NeuN (marker of neuronal nuclei), CDP (cortical upper layers), FoxP2 (cortical deeper layers), GABA (interneurons) and the astroglial marker S100 β (Fig. 4C–H). Similar cellular constituents have also been

found in nodules from postmortem human PH brains with FLNA mutations (21–23).

Disruption of radial glia in FlnA-knockdown rats

Radial glia plays a critical role in the construction of the cerebral cortex by providing a scaffold for radial migration of new neurons to their target locations (24). Therefore, we investigated the influence of FlnA knockdown on radial glia organization. Brains transfected with RFP alone or together with 3UTRshp were immunostained 2 and 5 days post-electroporation with the radial glial marker vimentin. In most of E17 and in all E20 FlnA-knockdown brains, but not in age-matched controls, we observed a disruption of radial glial fibers in the VZ/SVZ, where RFP-positive cells accumulate forming heterotopia (Fig. 5A–H). To further examine the role of FlnA in radial glial cells, *in utero* RNAi experiments were performed with a brain lipid-binding protein (BLBP)-promoter driving GFP expression construct specific

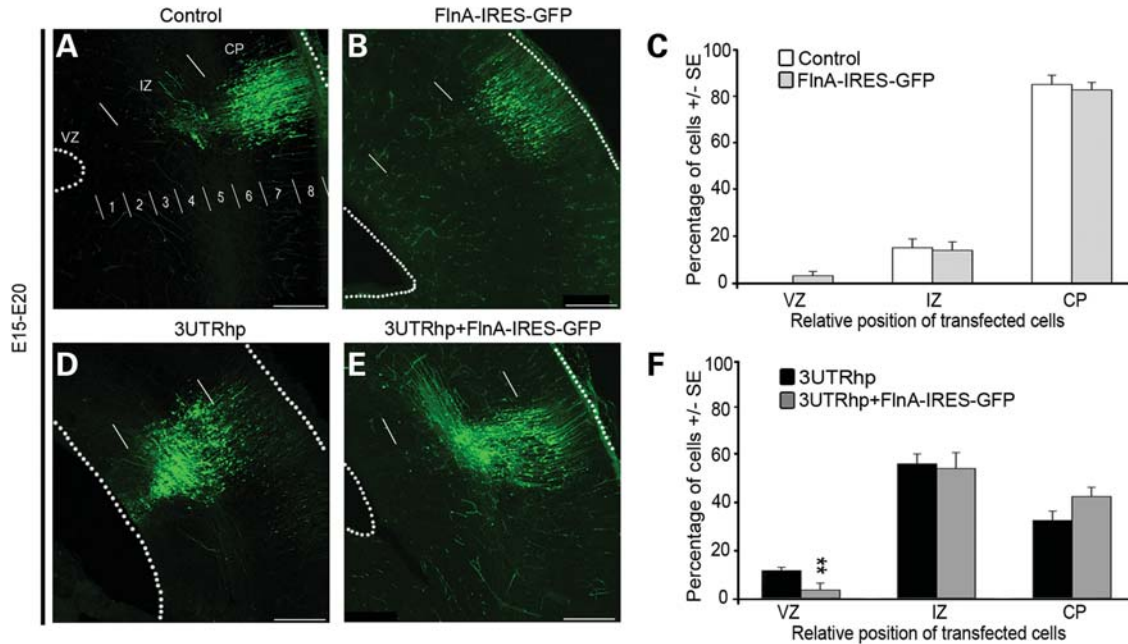


Figure 3. Expression of full-length FlnA rescues the radial migration defect of FlnA-knockdown cortical neurons. (A and B) Representative coronal sections of E20 rat brains 5 days after electroporation with either pCAGIG empty vector (or Control) (A) or FlnA-IRES-GFP construct (B). (C) Quantification (means \pm SEM) of GFP-positive cell distribution in the VZ (strata 1, 2), the IZ (strata 3–5) and the cortical plate (CP = strata 6–8) of independent brains at E20 (Control, $n = 10$; FlnA-IRES-GFP, $n = 9$) and expressed as a percentage of the total. Five days after electroporation, the majority of GFP-positive cells have reached the cortical plate of control ($84.1 \pm 3.4\%$) and FlnA-IRES-GFP-transfected brains ($83.3 \pm 4.05\%$). (D and E) Rescue experiment was performed using 3UTRhp combined with pGAGIG empty construct (D), or combined with FlnA-IRES-GFP (E). (F) Quantification (means \pm SEM) of GFP-positive cell distribution in the cortices of E20 independent brains, electroporated 5 days earlier with either 3UTRhp ($n = 12$) or FlnA-IRES-GFP combined with 3UTRhp ($n = 6$). ** $P < 0.01$ when compared with 3UTRhp.

for those cells. In E17 control brains ($n = 10$), electroporated at E15 and immunostained with anti-GFP and anti-vimentin antibodies, GFP/vimentin-positive cells displayed the characteristic features and polarized morphology of radial glia with processes extending from the VZ (Fig. 5I–K) to the pial surface (Fig. 5O). In contrast, in age-matched FlnA-knockdown brains ($n = 10$), several GFP/vimentin-positive cells no longer displayed typical features of radial glia and exhibited misoriented apical processes (Fig. 5L–N). However, basal processes remain attached to the pial surface (Fig. 5P). Apical endfeet of radial glial cells form an adhesive lining at the VZ (25), thus defects in this structure could contribute to PH formation. Furthermore, $\beta 1$ -integrins are involved in radial glial endfeet anchoring to the ventricular surface (26,27). These anchors are reinforced by cadherin–catenin-based adherens junctions, which attach apical endfeet of adjacent radial glial cells to each other to maintain the neuroepithelial integrity of the VZ (25). We therefore examined whether there was an alteration of the neuroepithelial lining in FlnA-knockdown brains, 2 and 5 days post-electroporation, by $\beta 1$ -integrin and β -catenin immunostainings. At E17, we detected alterations in the neuroepithelial lining in most of FlnA-knockdown brains as indicated by a discontinuity in β -catenin and $\beta 1$ -integrin stainings in the VZ (Fig. 5S and T). In comparison, in all age-matched controls, the VZ was characterized by tight cell associations (Fig. 5Q and R). Disruption of the neuroepithelial lining was even more marked below the heterotopia in the majority of E20 FlnA-knockdown brains (Fig. 5U–X). Our data suggest

that disruption of both polarized radial glial scaffold and neuroepithelial lining was the likely cause of the failure of some neurons to migrate away from the VZ and forming PH.

Role of FlnA in neural progenitor cell proliferation

In addition to providing guidance, radial glia also function as neural progenitors, giving rise to most cortical neurons (28,29). To study the effect of FlnA knockdown during neural progenitor cell-cycle progression, brains that were transfected at E15 with RFP alone or combined with 3UTRhp or 3UTRm3hp were stained 48 h post-electroporation for the proliferation marker Ki-67. In control brains transfected with RFP alone ($n = 7$ embryos) or together with 3UTRm3hp ($n = 5$ embryos), $38.4 \pm 4.3\%$ or $37.3 \pm 5.9\%$ of RFP-expressing cells in the VZ were Ki67-positive, respectively (Fig. 6A, C and D). Surprisingly, the percentage of Ki67-positive cells in 3UTRhp transfected brains ($15.9 \pm 2.9\%$, $n = 5$ embryos) was significantly decreased ($P < 0.01$) (Fig. 6B and D). Similar results were obtained with the anti-phosphovimentin antibody 4A4, which labels M-phase neural progenitor cells. Indeed, we found in 3UTRhp brains ($n = 9$ embryos) that only $12.4 \pm 2.1\%$ ($P < 0.05$) of transfected cells were positive for 4A4 compared with control brains transfected with RFP ($27.4 \pm 7.1\%$; $n = 6$ embryos) or 3UTRm3hp ($28.1 \pm 4.8\%$; $n = 6$ embryos) (Fig. 6E–H). These data indicate that knockdown of FlnA impaired the progression of neural progenitors through the cell cycle. To determine whether this effect induced a

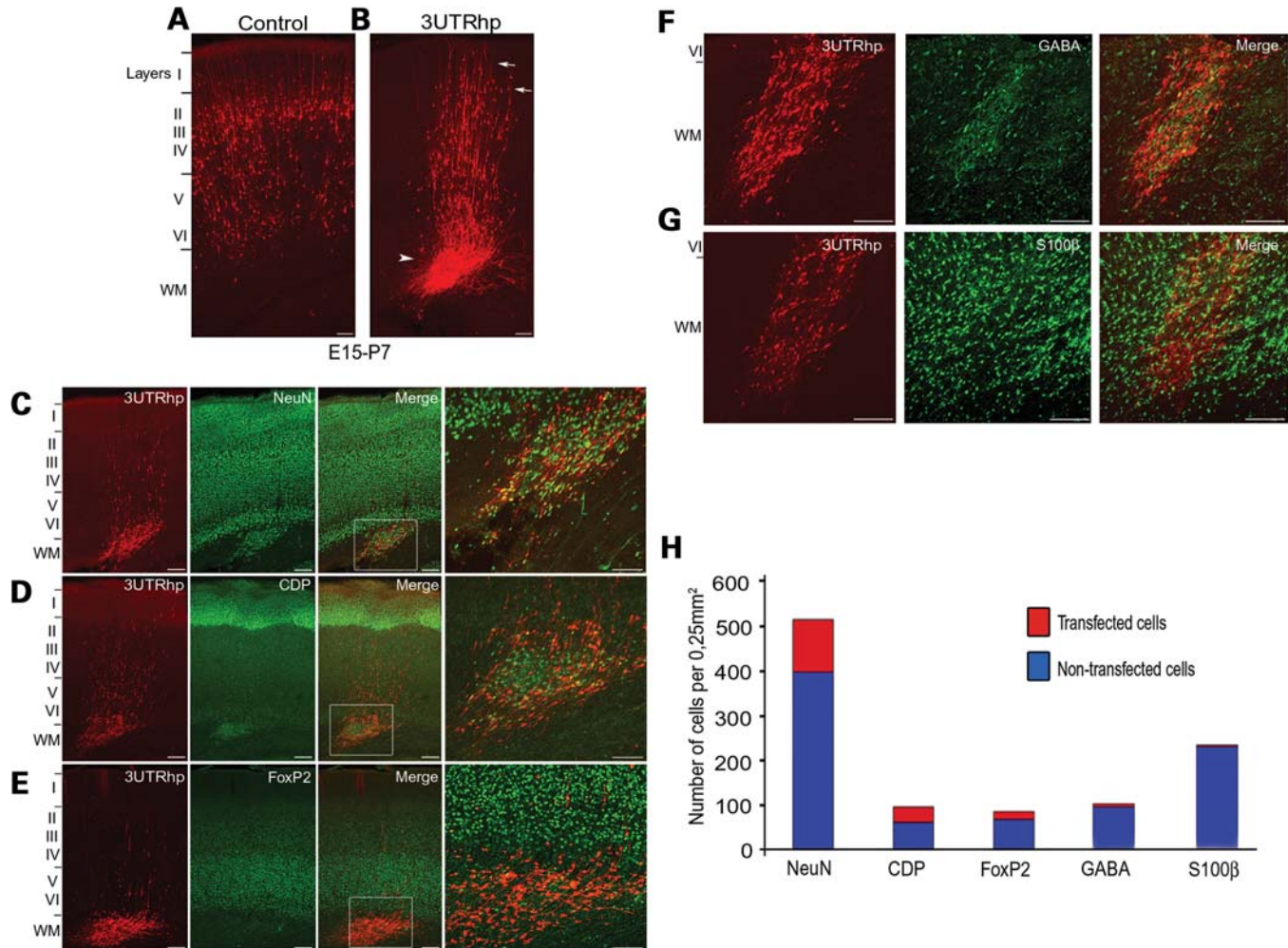


Figure 4. Knockdown of FlnA leads to the formation of PH in P7 rat pup brains. (A and B) Representative neocortical sections showing the laminar position of transfected cells in rats electroporated at E15 with either RFP construct alone (or control) (A) or combined with 3UTRhp (B) and analyzed postnatally at P7. In control brain, RFP-positive cells are mainly found in layers II/III/IV of the neocortex (A). In contrast, in 3UTRhp brains, several transfected cells formed an ectopic mass near the ventricular surface (arrowheads). Numerous transfected cells (arrows) extend out of the heterotopia into all neocortical layers (B). (C–E) Immunostaining of 3UTRhp brain sections at P7 revealed the presence of both transfected and non-transfected cells that were immunopositive for the neuronal marker NeuN (C), cortical upper layers marker CDP (D) and the deeper layers marker FoxP2 (E). High-magnification views of the boxed sections in merged images show both transfected and non-transfected neurons. (F and G) Heterotopia also contained several interneurons labeled with GABA marker (F) and many differentiated astrocytes positive for S100β (G). (H) Number of transfected and non-transfected NeuN+, CDP+, FoxP2+ neurons, GABA+ interneurons and S100β+ astrocytes in a surface area of 0.25 mm² which represents the average nodule size. Scale bars: 500 μm (A, B, C, D and E); 100 μm (F, G and high-magnification insets in C, D and E).

premature neuronal differentiation, we examined the proportion of electroporated cells in the VZ at E15 that expressed the early neural marker TuJ1 2 days later. Whereas in control brains (RFP, $n = 3$; or 3UTRm3hp, $n = 3$) none of the transfected cells in the VZ was positive for TuJ1, we observed that $5.3 \pm 2\%$ ($P < 0.05$) of RFP-positive cells co-expressed TuJ1 in 3UTRhp-transfected brains ($n = 3$) (data not shown). Alteration in neural progenitor cell-cycle progression induced by FlnA knockdown could also result in an increase of cell death. To investigate this issue, 3UTRhp-transfected brains were immunostained for cleaved caspase-3. No obvious change in cell death was noted between 3UTRhp-transfected brains ($n = 3$) and control brains ($n = 3$; data not shown). Taken together, these experiments suggest that FlnA might regulate cell-cycle progression of cortical neural progenitors.

FLNA-related PH in humans results from alterations of radial glia

To evaluate whether, in humans, FLNA-related PH resulted from alterations in radial glia organization and function, we investigated postmortem brains of two female patients harboring a different FLNA mutation. Patient 1 was a 35-week-old fetus with a prenatal detection of PH by brain MRI. At autopsy, the fetus displayed no dysmorphic features or extracerebral abnormalities. Patient 2 was a 3-month-old child who presented severe congenital heart and lung disease and died from respiratory distress. Neuropathological analysis of both patients showed the presence of bilateral PH (Fig. 7A–D). Sequencing of the *FLNA* gene in patient 1 revealed a substitution of a cytosine for a thymine at nucleotide position 691 in exon 4 that generates a stop codon at

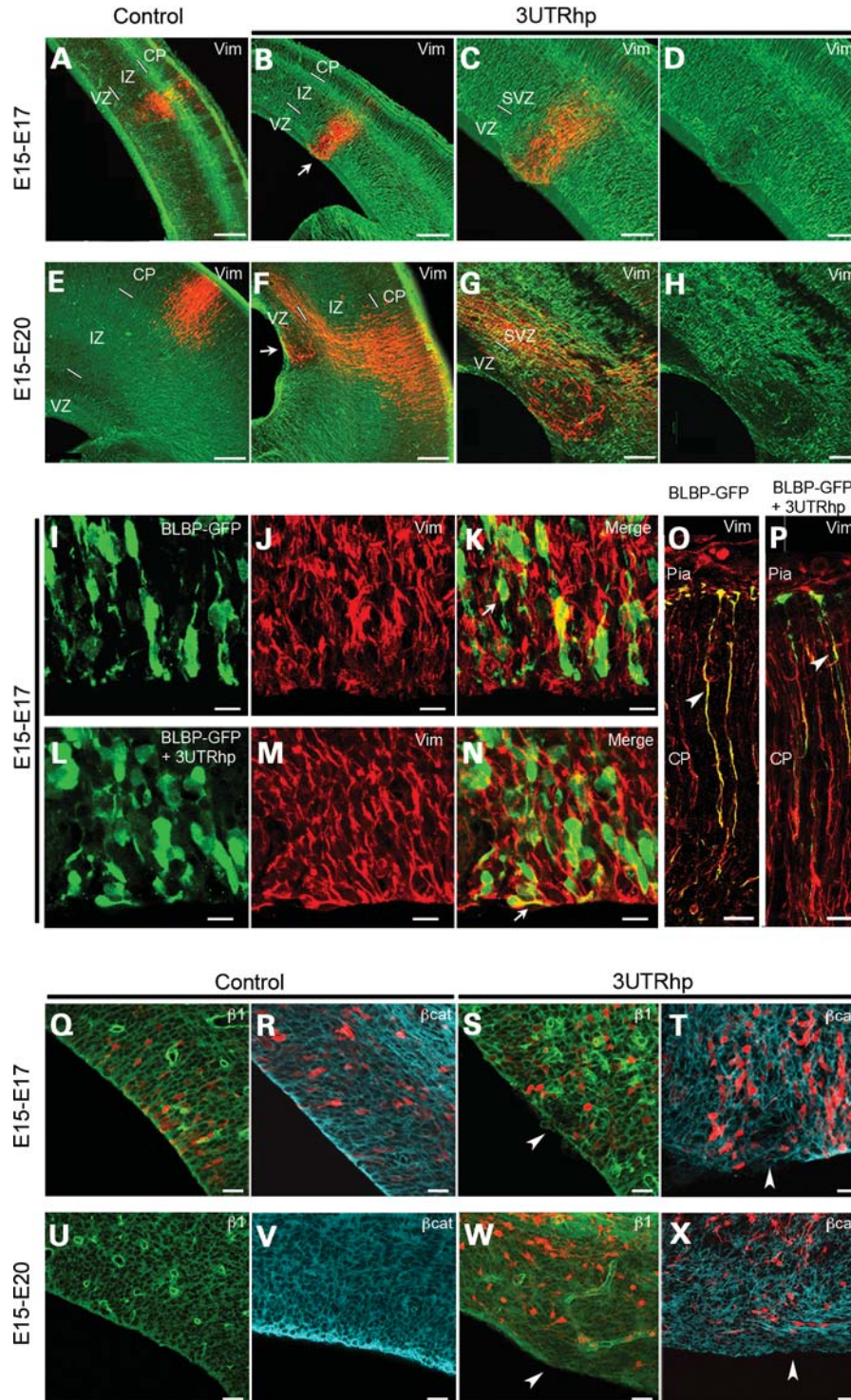


Figure 5. Genesis of PH mediated by FlnA knockdown is linked to radial glia disruption. (A–H) Representative coronal sections of E17 (A–D) or E20 (E–H) rat brains transfected at E15 with either RFP alone (control) or combined with 3UTRhp and immunostained for vimentin (in green). In 3UTRhp brain sections at E17 (B, C and D) and E20 (F, G and H) compared with age-matched controls (A and E), vimentin staining revealed a marked disruption of radial glial apical fibers. (C, D, G and H) Higher magnifications of regions indicated by an arrow in (B) and (F). (I–N) Higher magnification confocal images of E17 rat cortices transfected at E15 with the BLBP-GFP construct alone (control; I–K) or combined with 3UTRhp (L–N) and immunostained for GFP (green) and vimentin (red) to highlight radial glial cells (J, K, M and N). The organization and orientation of GFP+/vimentin+ cells are altered in the VZ of FlnA-knockdown brain (arrow in N) compared with control (arrow in K). (O–P) High-magnification representative images showing that pial processes in 3UTRhp brain section (P) resemble to those observed in control (O). (Q–X) Representative neocortical sections showing E17 and E20 brains transfected with RFP alone (control) or combined with 3UTRhp and immunostained for β 1-integrin (Q, S, U and W) or β -catenin (R, T, V and X) markers. In the VZ of 3UTRhp brains, β 1-integrin (S and W) and β -catenin (T and X) staining was discontinuous along the neuroepithelial lining (arrowheads) in regions where RFP-positive cells accumulate. Scale bars: 200 μ m (A, B, E and F); 100 μ m (C, D, G and H); 50 μ m (I–X).

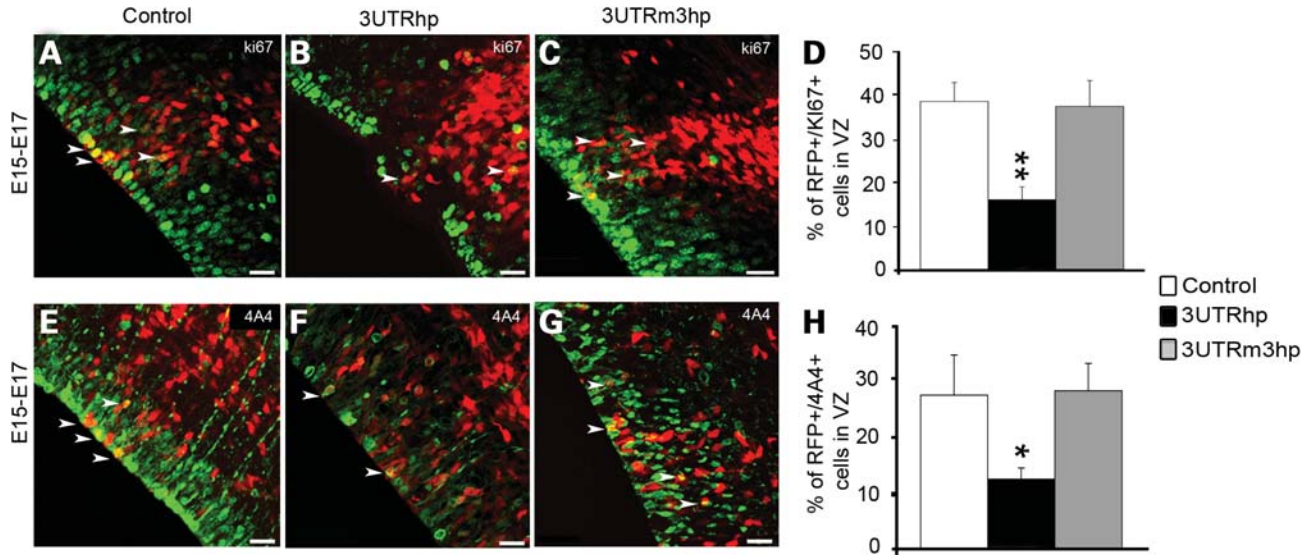


Figure 6. FlnA is required for cell-cycle progression of cortical progenitors. (A–C and E–G) Representative confocal images of the ventricular zone (VZ) of rat cortices transfected at E15 with RFP alone or combined with 3UTRhp or with 3UTRm3hp and immunostained 40–42 h later with the proliferation marker Ki67 (green) (A–C) or with the M-phase marker phosphovimentin (4A4, green) (E, F and G). Transfected cells positive for either marker appeared in yellow (arrows). (D and H) Quantification (means \pm SEM) of RFP and Ki67 (D) or RFP and 4A4 (H) double-positive transfected cells in the VZ of independent brains (for Ki67, RFP: $n = 7$ embryos; 3UTRhp: $n = 5$ embryos; 3UTRm3hp: $n = 5$ embryos and for 4A4, RFP: $n = 6$ embryos; 3UTRhp: $n = 9$ embryos; 3UTRm3hp: $n = 6$ embryos). The percentage of total RFP-transfected cells that were positive for Ki67 or 4A4 was significantly reduced in FlnA knockdown brains compared with control or 3UTRm3hp. * $P < 0.05$, ** $P < 0.01$ when compared with control and 3UTRm3hp (D and H). Scale bars: 50 μ m.

amino acid position 231 (Q231X) (Fig. 7E). In patient 2, a cytosine insertion was identified at nucleotide 6306 in exon 39, causing a translational frameshift that introduced 56 novel amino acids before premature termination (R2103QfsX56) (Fig. 7E). These two novel FLNA mutations are predicted to delete the C-terminal dimerizing domain as well as the β -class integrins interaction domains. Because most ependymal cells derived from radial glia (30), the neuroependymal integrity was assessed in our patients. We found that heterozygous loss of FLNA disrupted the neuroependymal lining as revealed by the altered distribution of vimentin (Fig. 7H, I, L and M) and GFAP (data not shown) at the ventricular surface. Moreover, these mutations induced the loss of ependymal cells in regions immediately below PH (Fig. 7P, Q, T and U), the few remaining cells being strongly labeled by β 1-integrin (Fig. 7Q and U). In contrast, in age-matched control brains, vimentin (Fig. 7F, G, J and K) and GFAP (data not shown) staining highlighted the neuroependyma lining characterized by tight cell-associations, as β 1-integrin labeling was restricted to the basal membrane of vessels (Fig. 7N, O, R and S). Additionally, in controls, we identified vimentin-immunopositive fibers that resemble radial glial processes that were sparse in fetuses (Fig. 7F and G) or absent in child (Fig. 7J and K). In contrast, in both patients, we found disorganized fibers around PH that were dense and strongly stained for vimentin (Fig. 7H, I, L and M). Our findings suggest that both the presence of these fibers around PH and the disruption of neuroependyma are due to alterations of radial glia function and further maturation into ependymal cells. Overall, these observations are reminiscent of the phenotype of FlnA-knockdown rats.

FlnA-knockdown rats display increased susceptibility to PTZ-induced seizures

Epilepsy is the main presenting symptom of patients with PH due to FLNA mutations (6). Therefore, we investigated whether FlnA-knockdown rats displayed an increased susceptibility to seizures. One of the commonly used behavioral ways to study brain excitability is the application of PTZ, which is a chemical convulsant that induces seizures by blocking the GABAA receptor-coupled chloride ionophore (31). Thus, FlnA-knockdown rats at P30 and age-matched control rats (transfected with RFP alone) were intraperitoneally injected with subconvulsive doses of PTZ (25 mg/kg) every 10 min. Injections of PTZ were continued until each rat had a generalized tonic-clonic seizure. Generalized seizures in the FlnA-knockdown rats ($n = 11$) occurred at significantly lower doses of PTZ (Fig. 8A) and with significantly shorter latencies (Fig. 8B) than they did in controls ($n = 9$; Fig. 8A and B). In addition, 3 out of 11 FlnA-knockdown rats died after seizures (Fig. 8C). Next, these animals were processed for histological analyses in order to detect ectopic nodules. Immunohistochemical analyses were performed on coronal brain sections with neuronal markers (NeuN, CDP, FOXP2 and GABA) and a glial-specific marker (S100 β). This allowed us to confirm the presence of heterotopic neurons dispersed or organized into nodules ($>0.17 \text{ mm}^2$) adjacent to the lateral ventricular wall in FlnA-knockdown brains. Then, we investigated whether there was a correlation between the PH size and susceptibility to seizures. Although all FlnA-knockdown rats displayed PTZ-induced seizures, we found no correlation between their occurrence and the extent of PH (data not shown). Finally, our data suggest that lowered

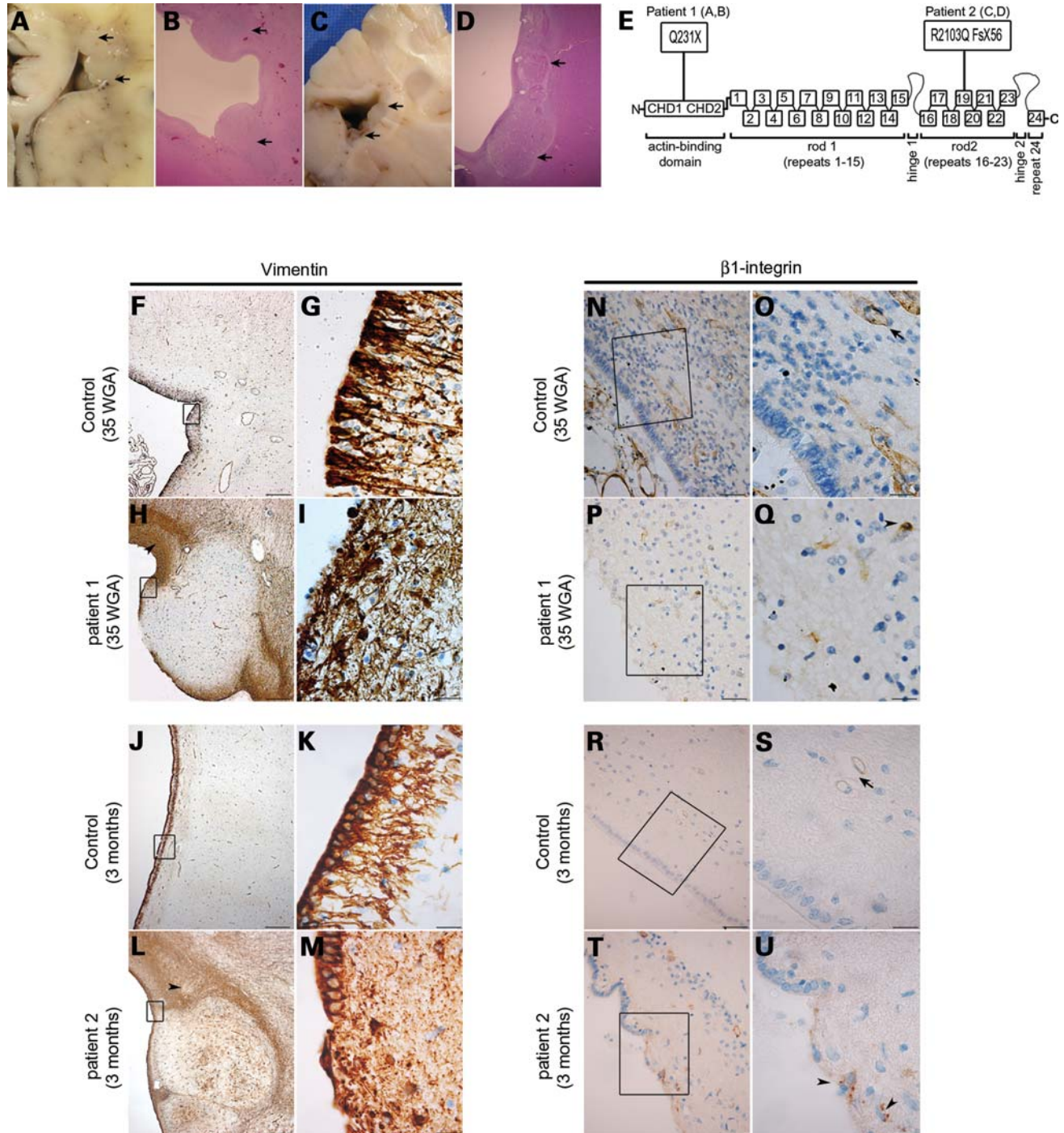


Figure 7. Alteration of the radial glia scaffold in human PH brains at different ages harboring distinct FLNA mutations. (A and C) Macroscopic appearance of nodular heterotopia in postmortem brains of a 35-week female fetus (A; patient 1) and a 3-month-old female child (C; patient 2). Note the small protrusions into the ventricle from the lateral wall (arrows). (B and D) Hematoxylin and eosin stainings show, in both patients, the lateral ventricle with contiguous nodules (arrows) along its lateral border. (E) Schematic representation of the FLNA protein showing the position of the Q231X and the R2103QfsX56 heterozygous FLNA mutation identified in patient 1 and patient 2, respectively. (F–M) Photomicrographs of brain tissue sections from 35 weeks' gestational age control fetuses (F and G), a 3-month-old control child (J and K) and PH patients 1 (H and I) and 2 (L, M) immunostained with the radial glial marker vimentin. In control fetuses, vimentin staining highlights the radial glial architecture (G), whereas in control child it is mainly restricted to ependymal cells lining the ventricle (K). In contrast, in brain sections from both PH patients, the radial glial scaffold appears dense (arrowhead) and is disorganized in the ventricular zone around PH (H and L). High magnifications (G and K) of areas outlined in (F) and (J) show the integrity of neuroependyma in controls, whereas high magnifications (I and M) of areas outlined in (H) and (L) reveal the disruption of the neuroependymal lining and loss of ependymal cells along PH. (N–U) Photomicrographs of β 1-integrin staining along the ventricular wall in controls (N and R) and in both PH patient (P and T) brains demonstrated disruption in cell–cell junctions and in neuroepithelial lining below nodular heterotopia. Areas outlined in (P) and (T) point to ependymal cells shown at higher magnification in (Q) and (U), respectively. Note that few cells below PH were strongly stained by β 1-integrin (arrowhead in U and Q). In comparison, in control brains, higher magnifications (O and S) of areas outlined in (N) and (R) show that β 1-integrin staining is mainly restricted to the basal membrane of vessels (arrow in O and S). Scale bars: 500 μ m (F, H, J and L); 100 μ m (N, P, R and T); 50 μ m (G, I, K, M, O, Q, S and U).

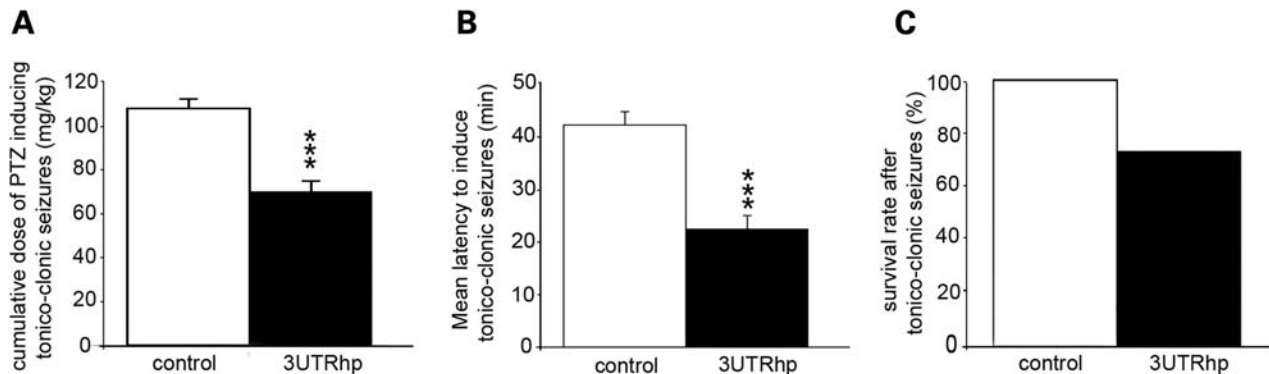


Figure 8. Increased susceptibility to PTZ-induced seizures in FlnA knockdown rats at P30. (A and B) Quantification of doses of PTZ (A) and mean latency (B) to induce generalized tonic-clonic seizures in two groups of rats electroporated at E15: control or malformation free rats ($n = 9$) and FlnA-knockdown rats (3UTRhp, $n = 11$) displaying periventricular heterotopia. (C) Survival rate of control and FlnA-knockdown (or 3UTRhp) rats after generalized seizures. *** $P < 0.001$ when compared with control.

seizure threshold in FlnA-knockdown rats results from the presence of PH.

DISCUSSION

In this study, we show that embryonic knockdown of FlnA impairs radial migration by affecting radial glia organization and neuronal orientation in the upper IZ. We also demonstrate that PH, in postnatal brains, resulted from both cell autonomous and non-cell autonomous effects of FlnA knockdown. Specifically, non-transfected neurons and glial cells were observed within the ectopic nodules. Our findings indicate that defective neuronal migration alone is not sufficient to account for all of the hallmarks of PH and that pathogenesis might result from a disruption of the polarized radial glial scaffolding. Consistently, we found alterations in radial glia organization around FLNA-related PH in rats and humans. Moreover, similar disruption of radial glia organization has been previously observed in five human fetuses with PH from unknown etiology, suggesting that this feature may represent a common pathogenic mechanism of PH (32).

Radial glia are highly polarized cells that play an essential role during cortical development through their function as neural progenitors and guides of neuronal migration (24,25). Polarized radial glial cells are characterized by a pear-shaped cell soma in the VZ, with a short apical process that forms an endfoot anchored to the ventricle and a long, slender basal process extending to the pial surface (33). The basal process serves as a scaffold for the migration of newborn neurons (34). In contrast, the apical processes of adjacent radial glial cells are attached to one another via adherens junctions to maintain their apical attachment and the neuroepithelial integrity of the VZ (25). Adherens junctions are multiprotein complexes composed of cadherins and α - and β -catenin. The latter binds to the cadherin cytoplasmic domain and provides a connection to the actin cytoskeleton by interacting with α -catenin (35). Apical adherens junctions are also necessary for the establishment of the apical-basal polarity in radial glial cells (36). In addition β 1-integrin proteins, through their interaction with laminin α -2 chain, which serve as ligands for integrins in the extracellular matrix, reinforce radial glial

apical endfeet anchoring at the ventricular surface (37). A recent study has shown that inhibition of β 1-integrin function at the VZ results in apical endfeet detachment (27). Although we found that FlnA is specifically expressed in the VZ during embryonic cerebral cortical development, its function in radial glial apical endfeet adhesion remains unclear. It has been shown that β 1-integrin-mediated cell adhesion to the extracellular matrix is dependent on the binding of FLNA to vimentin and protein kinase-C epsilon (PKC ϵ) (38). The formation of this multiprotein complex allows vimentin phosphorylation by PKC ϵ (39,40). This step is crucial for the activation and trafficking of β 1-integrin to the plasma membrane but also for cell migration (39,41). Indeed, fibroblasts obtained from PKC ϵ -knockout mice exhibit defective cell adhesion and motility (42). Similarly, knockdown of FLNA in HEK cells abrogated vimentin phosphorylation and reduced cell surface β 1-integrin expression (38). Based on these observations, alterations of the FLNA/ β 1-integrin pathway may contribute to PH pathogenesis. Supporting this proposed mechanism, we found that fibroblast lysates of patients with PH and FLNA mutation showed lower levels of phosphorylated vimentin (data not shown). More interestingly, we showed that the distribution of β 1-integrin was altered at the ventricular surface in FlnA-knockdown rats and in our PH patients whose identified Q231X and R2103QfsX56 mutations are predicted to alter FLNA/ β 1-integrin interaction (43). Consequently, the loss of the polarized localization of β 1-integrin as well as β -catenin affects neuroepithelial lining integrity in regions immediately below PH. These data, consistent with previous studies (14,23), support a major role of FLNA in cell-cell adhesion and polarity of radial glial cells. Furthermore, we observed that the FLNA frameshift mutation identified in our PH patient influences the adhesiveness of radial glial endfeet and the transition from radial glial cells to adult ependymal cells, leading to neuroependymal disruption. Indeed, it has been shown that radial glial cells retract their basal process but retain adherens junctions to form the lining of the postnatal ventricles as ependymal cells (30). Taken together, these findings suggest that FLNA is important for the development and the maintenance of the radial glial scaffold during corticogenesis.

In addition to their structural role, radial glial cells also function as neuronal progenitors (28) and have been identified as a major source of neurons during development (29). Radial progenitors can either divide symmetrically to self-renew or divide asymmetrically to produce another radial progenitor and either a neuron or an intermediate progenitor daughter cell (IPC) (44,45). Whereas radial progenitors divide at the apical surface of the VZ, IPCs populate the overlying SVZ, where they divide symmetrically to generate neurons for the upper cortical layers (45). To our surprise, we found that knockdown of FlnA expression in neural progenitors affects their progression through the cell cycle and leads to significant increase in the proportion of newly generated neurons. Consistent with this observation, FlnA-null mutant mouse embryonic stem cells or cortical neural progenitors are also able to differentiate into neurons *in vitro* (14). From our data, alterations in cell proliferation following knockdown of FlnA are most likely due to the disruption of radial glial cell adhesion. This hypothesis is supported by several studies showing that disruption of apical adherens junctions between radial glial cells can result in defects in cell proliferation. Indeed, inactivation of α E-catenin or β -catenin signaling in the developing nervous system disrupts adherens junctions and causes cortical progenitor cells to prematurely exit the cell cycle and differentiate into neurons (46,47). Our results showed a discontinuous staining of β -catenin in the VZ of FlnA-knockdown brains; however, a direct association of FLNA with β -catenin has never been characterized. Interestingly, a recent study showed that the RhoA protein, an FLNA partner, is essential for the maintenance of adherens junctions and constrained proliferation of neural progenitors in the developing mammalian brain (48). Based on these findings, we propose that disruption of adherens junctions following FlnA knockdown may result in neural progenitor cells delaminating from the VZ, thus influencing their cell-cycle progression.

Approximately 88% of PH patients with FLNA mutations have focal epilepsy, which can begin at any age (6). The seizures may range in severity from mild, with rare frequency and remission without the need of antiepileptic drugs, to intractable (6). Functional MRI studies suggest that PH can be functionally integrated in complex circuits and participate, for example, in motor activity (49). Depth electrode studies also showed the presence of complex circuits which underlie simultaneous seizure initiation within periventricular nodules and, at a distance, in the neocortex (50,51). Thus, progress in our understanding of mechanisms underlying epilepsy requires employment of an appropriate FlnA animal model. Though two FlnA knockout mice strains have been developed, progress has been hindered by the fact that none of them was epileptic and showed the presence of ectopic nodules (14,15). In contrast, *in utero* knockdown of FlnA expression has succeeded in reproducing a PH phenotype in rat similar to the one observed in human patients. Moreover, all juvenile FlnA-knockdown rats displayed an increased susceptibility to convulsive agents regardless of the extent of PH and even a few heterotopic neurons are sufficient to yield epilepsy. These observations are in agreement with previous clinical studies in patients with FLNA mutations that revealed no correlation between the extent of PH and epilepsy severity (6,52).

In summary, we have developed the first FlnA animal model reliably producing PH, improving our understanding of the molecular mechanism underlying heterotopia formation. Indeed, the mechanism of PH formation was originally seen as a defect in neuronal migration. Here, we provide evidence that impaired expression of FLNA in rodents and in humans leads to the disruption of the polarized radial glial scaffold in the ventricular zone, impairing radial glia functions as neural progenitors and guides of neuronal migration and giving rise to ectopic neuronal nodules. Moreover, we confirmed the reliability of this new model of PH by showing that juvenile FlnA-knockdown rats are highly susceptible to seizures. Thus, this animal model provides a unique opportunity to investigate the role of FLNA-related PH in the generation of seizures and therapeutic prospects.

MATERIALS AND METHODS

RNAi constructs

RNAi experiments were conducted with two shRNAs targeting the coding sequence (CDS_{hp}; nucleotides 5963–5983) or the 3'UTR (3UTR_{hp}; nucleotides 8269–8290) of *Rattus norvegicus* FlnA mRNA (Genbank accession number FJ416060). These constructs were designed using the siRNA Target Designer software (<http://www.promega.com/siRNADesigner/program>). BLAST searches against rat databases confirmed the specificity of each target. As negative controls, we used two corresponding non-targeting shRNAs (CDS_{m3hp} and 3UTR_{m3hp}) with the same nucleotide sequence except in three positions. These shRNAs were subcloned into an mU6pro vector (gift from Dr J. LoTurco). For rescue experiments, we subcloned the coding sequence of rat FlnA cDNA without the UTRs into pCAGIG vector (Addgene, Cambridge, MA, USA).

Cell culture and immunocytochemistry

Rat C6 glioma cells were maintained at 37°C in a humidified 5% CO₂ incubator in DMEM (Invitrogen) supplemented with 10% FBS, 1 mM L-glutamine and D-glucose. Cells were transfected with the Neon Transfection System (Invitrogen) or the Combimag reagent (OZ-Biosciences, France) according to the manufacturer's protocol and postfixed in Antigenfix solution (Diapath, Italy). Cells were blocked for 1 h at RT with 5% normal goat serum, 0.3% Triton X-100 in PBS and were incubated overnight with FlnA antibody (Santa Cruz, 1/500) at 4°C. Cells were analyzed on a laser-scanning confocal microscope (FluoView 300; Olympus).

RT-PCR and qPCR

Total RNA was isolated from C6 rat glial cells, using RNeasy-Plus Mini Kit, according to the manufacturer's protocol (Qiagen). cDNA was synthesized using the Quantitect Reverse Transcription Kit, according to the manufacturer's protocol (Qiagen). Quantitative PCR was performed using oligonucleotides specific for *R. norvegicus* FlnA (Qiagen, QT00374458) and *cyclophilinA* (Qiagen, QT00177394) as a control probe. Amplification was done using SYBR-Green

chemistry (Roche diagnostics) and Roche amplification technology (Light Cycler 480). All experiments were performed in triplicate.

Western blot analysis

Cells were lysed in a buffer (150 mM NaCl, 50 mM Tris-HCl, pH = 8.0, 50 mM NaF, 0.5% Nonidet P40, 2 mM EDTA, protease inhibitor cocktail) at 4°C before proteins were heat-denatured and processed by SDS-PAGE, transferred to nitrocellulose and immunoblotted with the following primary antibodies: FlnA (Santa Cruz, 1/1000), α -tubulin (Sigma, 1/10 000) and GFP (Chemokim, 1/5000). The proteins were detected with the Western Lumilight Kit chemiluminescence reagent (GE Healthcare).

In utero electroporation

Wistar rats (Janvier, France) were mated, cared for and used in our animal facilities in agreement with the European Union and French legislations. Timed pregnant rats (E15; E0 was defined as the day of confirmation of sperm-positive vaginal plug) were anesthetized with a mixture of ketamine/xylazine (respectively at 100 and 10 mg/kg). The uterine horns were exposed, and a lateral ventricle of each embryo was injected using pulled glass capillaries and a microinjector (Picospritzer II; General Valve Corporation, Fairfield, NJ, USA) with Fast Green (2 mg/ml; Sigma, St Louis, MO, USA) combined with the following DNA constructs: 0.5 μ g/ μ l pCAGGS-RFP either alone or with 1.5 μ g/ μ l of shRNA construct targeting the *FlnA* mRNA. Plasmids were further electroporated by discharging a 4000 μ F capacitor charged to 50 V with a BTX ECM 830 electroporator (BTX Harvard Apparatus, Holliston, MA, USA). The voltage was discharged in five electrical pulses at 950 ms intervals via 5 mm electrodes placed on the head of the embryo across the uterine wall. We performed *in utero* electroporation in embryonic rats at E15 corresponding to an active period of both radial and tangential migration of newborn neurons in the cortex.

Neuropathological procedures

Neuropathological analyses were performed on two infant brains (3 months old) and four fetal brains (35 gestational weeks) in accordance with French Law. Brains were removed 24 h after death and fixed in 10% (v/v) formaldehyde solution containing NaCl (9 g/l) and ZnSO₄ (3 g/l) for a variable time (depending on the brain volume) of at least 6 weeks. After macroscopic examination, selected blocks were paraffin-embedded, and 7 mm slices were stained with hematoxylin, cresyl violet and luxol fast blue. Immunohistochemistry was performed using a Ventana BenchMark XT immunostainer with the following antibodies: vimentin (Novocastra), β 1-integrin/CD29 (Epitomics, 1/50) and GFAP (Dako). Sections were imaged on a microscope (Nikon, Eclipse E800).

Immunohistochemistry

Rat brains were fixed (E17 or E20) or perfused (P7) with Antigenfix solution and sliced at 100 μ m on a vibratome (Microm). Slices were blocked at RT for 1 h with 5% normal goat serum, 0.3% Triton X-100 in PBS and incubated overnight at 4°C with the appropriate antibody for cell proliferation: Ki-67 (Chemicon, 1/300) and 4A4 (Phosphorylated-Vimentin-Ser55; MBL, 1/200); for neuronal differentiation: PSA-NCAM (gift from Dr Rougon, IBDML Marseille), TuJ1 (β -III tubulin; Promega, 1/6000), FOXP2 (Abcam, 1/4000), CDP (M-222 Santa Cruz, 1/200), Neu-N (Millipore, 1/300), GABA (Sigma, 1/8000), glial marker S100 β (EP1576Y Abcam, 1/1000) and Vimentin (Millipore, 1/300); for neuroependymal lining: FlnA (Epitomics, 1/1000), β -catenin (Transduction Laboratories, 1/300) and β 1-integrin (12G10 Millipore, 1/100); for cell death: Caspase3-Asp175 (Cell Signaling, 1/200). Sections were imaged on a laser-scanning confocal microscope (FluoView 300; Olympus).

Quantitative analysis

Quantification was performed with the eCELLence software (www.gvt.it/ecellence) on E17 and E20 coronal sections (100 μ m) located in the dorso-lateral neocortex. Relative positions of transfected cells were estimated by counting RFP-positive cells in eight areas of interest normalized in individual sections to fit within the whole thickness of the cortex. The latter was divided in three main regions corresponding to the ventricular zone (strata 1 and 2), the IZ (strata 3–5) and the cortical plate (strata 6–8). P7 coronal sections (100 μ m) were analyzed with the ImageJ software 1.44j. The nodule size was estimated in square-pixel with the ImageJ polygon tool and converted to mm². In the defined area, using the ImageJ plugin Cell Counter, we calculated the number of transfected and non-transfected cells that were positive for NeuN, CDP, FOXP2, GABA and S100 β markers. For cell-cycle progression, we counted the number of RFP-positive and RFP+/KI67+ cells or RFP-positive and RFP+/4A4+ cells in a defined area of 0.21 mm² (Adobe Photoshop-CS3) within the VZ of three confocal optical sections per embryo. For orientation analysis, we estimated the number of cells oriented between 0–45° and 45–90° in a defined area of 0.21 mm² within the IZ (Adobe Photoshop-CS3).

Seizure induction with PTZ

To evaluate the susceptibility to seizures in controls rats (RFP-transfected brains) and in FLNA-knockdown animals at P30, PTZ (25 mg/kg; Sigma) was administered via intraperitoneal injections every 10 min until generalized seizures occurred. Rats were placed in a plexiglass cage and the time to the onset of the generalized seizure was video-recorded. There was no significant difference in weight or sex-ratio between groups of animals. Experiments were blind: the phenotype of animals was established by morphological analysis after PTZ induction.

Statistical data

Statistical analysis was performed with SigmaStat (Systat Software, Chicago, IL, USA). A two-sample Student's *t*-test was used to compare means of two independent groups if the distribution of the data was normal. When the normality test failed, the non-parametric Mann–Whitney test was used. The one-way ANOVA all-Tukey test was used to compare multiple groups.

SUPPLEMENTARY MATERIAL

Supplementary Material is available at *HMG* online.

ACKNOWLEDGEMENTS

The authors wish to thank Dr J.B. Manent, Dr M. Colonnese and Professor K. Dudley for critical reading and input to our manuscript. We gratefully acknowledge the help of Dr H. Becq; Dr A. Falace; Dr F. Watrin (Scientific Manager of PPGI Platform) and Dr F. Michel (Scientific Adviser of INMAGIC Platform).

Conflict of Interest statement. None declared.

FUNDING

This work was supported by funding from INSERM, ANR (ANR-06-NEURO-08-01 contract number RPV06055ASA), European Union 6th Framework Thematic Priority Life Sciences, Genomics and Biotechnology for Health (EPICURE-contract number: LSH-CT-2006-037315) and the Federation des Maladies Orphelines (FMO). A.C. is supported by a PhD fellowship from Provence-Alpes-Côte d'Azur region and INSERM.

REFERENCES

- Kuzniecky, R.I. and Jackson, G.D. (2005) *Magnetic Resonance in Epilepsy*, 2nd edn. Elsevier, Burlington.
- Eksioglu, Y.Z., Scheffer, I.E., Cardenas, P., Knoll, J., DiMario, F., Ramsby, G., Berg, M., Kamuro, K., Berkovic, S.F., Duyk, G.M. *et al.* (1996) Periventricular heterotopia: an X-linked dominant epilepsy locus causing aberrant cerebral cortical development. *Neuron*, **16**, 77–87.
- Barkovich, A.J., Kuzniecky, R.I., Jackson, G.D., Guerrini, R. and Dobyns, W.B. (2005) A developmental and genetic classification for malformations of cortical development. *Neurology*, **65**, 1873–1887.
- Fox, J.W., Lamperti, E.D., Eksioglu, Y.Z., Hong, S.E., Feng, Y., Graham, D.A., Scheffer, I.E., Dobyns, W.B., Hirsch, B.A., Radtke, R.A. *et al.* (1998) Mutations in filamin 1 prevent migration of cerebral cortical neurons in human periventricular heterotopia. *Neuron*, **21**, 1315–1325.
- Sheen, V.L., Dixon, P.H., Fox, J.W., Hong, S.E., Kinton, L., Sisodiya, S.M., Duncan, J.S., Dubeau, F., Scheffer, I.E., Schachter, S.C. *et al.* (2001) Mutations in the X-linked filamin 1 gene cause periventricular nodular heterotopia in males as well as in females. *Hum. Mol. Genet.*, **10**, 1775–1783.
- Parrini, E., Ramazzotti, A., Dobyns, W.B., Mei, D., Moro, F., Veggiotti, P., Marini, C., Brilstra, E.H., Dalla Bernardina, B., Goodwin, L. *et al.* (2006) Periventricular heterotopia: phenotypic heterogeneity and correlation with Filamin A mutations. *Brain*, **129**, 1892–1906.
- Parrini, E., Mei, D., Wright, M., Dorn, T. and Guerrini, R. (2004) Mosaic mutations of the FLN1 gene cause a mild phenotype in patients with periventricular heterotopia. *Neurogenetics*, **5**, 191–196.
- Guerrini, R., Mei, D., Sisodiya, S., Sicca, F., Harding, B., Takahashi, Y., Dorn, T., Yoshida, A., Campistol, J., Krämer, G. *et al.* (2004) Germline and mosaic mutations of FLN1 in men with periventricular heterotopia. *Neurology*, **63**, 51–56.
- Sheen, V.L., Feng, Y., Graham, D., Takafuta, T., Shapiro, S.S. and Walsh, C.A. (2002) Filamin A and Filamin B are co-expressed within neurons during periods of neuronal migration and can physically interact. *Hum. Mol. Genet.*, **11**, 2845–2854.
- Nakamura, F., Osborn, T.M., Hartemink, C.A., Hartwig, J.H. and Stossel, T.P. (2007) Structural basis of filamin A functions. *J. Cell Biol.*, **179**, 1011–1025.
- Stossel, T.P., Condeelis, J., Cooley, L., Hartwig, J.H., Noegel, A., Schleicher, M. and Shapiro, S.S. (2001) Filamins as integrators of cell mechanics and signalling. *Nat. Rev. Mol. Cell Biol.*, **2**, 138–145.
- Cunningham, C.C., Gorlin, J.B., Kwiatkowski, D.J., Hartwig, J.H., Janmey, P.A., Byers, H.R. and Stossel, T.P. (1992) Actin-binding protein requirement for cortical stability and efficient locomotion. *Science*, **255**, 325–327.
- Nagano, T., Morikubo, S. and Sato, M. (2004) Filamin A and FILIP (Filamin A-Interacting Protein) regulate cell polarity and motility in neocortical subventricular and intermediate zones during radial migration. *J. Neurosci.*, **24**, 9648–9657.
- Feng, Y., Chen, M.H., Moskowitz, I.P., Mendonza, A.M., Vidali, L., Nakamura, F., Kwiatkowski, D.J. and Walsh, C.A. (2006) Filamin A (FLNA) is required for cell-cell contact in vascular development and cardiac morphogenesis. *Proc. Natl Acad. Sci. USA*, **103**, 19836–19841.
- Hart, A.W., Morgan, J.E., Schneider, J., West, K., McKie, L., Bhattacharya, S., Jackson, I.J. and Cross, S.H. (2006) Cardiac malformations and midline skeletal defects in mice lacking filamin A. *Hum. Mol. Genet.*, **15**, 2457–2467.
- Sarkisian, M.R., Bartley, C.M., Chi, H., Nakamura, F., Hashimoto-Torii, K., Torii, M., Flavell, R.A. and Rakic, P. (2006) MEKK4 signaling regulates filamin expression and neuronal migration. *Neuron*, **52**, 789–801.
- Saito, T. and Nakatsuji, N. (2001) Efficient gene transfer into the embryonic mouse brain using *in vivo* electroporation. *Dev. Biol.*, **240**, 237–246.
- Bai, J., Ramos, R.L., Ackman, J.B., Thomas, A.M., Lee, R.V. and LoTurco, J.J. (2003) RNAi reveals doublecortin is required for radial migration in rat neocortex. *Nat. Neurosci.*, **6**, 1277–1283.
- Jaglin, X.H., Poirier, K., Saillour, Y., Buhler, E., Tian, G., Bahi-Buisson, N., Fallet-Bianco, C., Phan-Dinh-Tuy, F., Kong, X.P., Bomont, P. *et al.* (2009) Mutations in human beta-2b tubulin result in asymmetrical polymicrogyria. *Nat. Genet.*, **41**, 746–752.
- Leviit, P., Cooper, M.L. and Rakic, P. (1981) Coexistence of neuronal and glial precursor cells in the cerebral ventricular zone of the fetal monkey: an ultrastructural immunoperoxidase analysis. *J. Neurosci.*, **1**, 27–39.
- Kakita, A., Hayashi, S., Moro, F., Guerrini, R., Ozawa, T., Ono, K., Kameyama, S., Walsh, C.A. and Takahashi, H. (2002) Bilateral periventricular nodular heterotopia due to filamin 1 gene mutation: widespread glomeruloid microvascular anomaly and dysplastic cytoarchitecture in the cerebral cortex. *Acta Neuropathol.*, **104**, 649–657.
- Thom, M., Martinian, L., Parnavelas, J.G. and Sisodiya, S.M. (2004) Distribution of cortical interneurons in grey matter heterotopia in patients with epilepsy. *Epilepsia*, **45**, 916–923.
- Ferland, R.J., Batiz, L.F., Neal, J., Lian, G., Bundock, E., Lu, J., Hsiao, Y.C., Diamond, R., Mei, D., Banham, A.H. *et al.* (2009) Disruption of neural progenitors along the ventricular and subventricular zones in periventricular heterotopia. *Hum. Mol. Genet.*, **18**, 497–516.
- Ayala, R., Shu, T. and Tsai, L.H. (2007) Trekking across the brain: the journey of neuronal migration. *Cell*, **128**, 29–43.
- Götze, M. and Huttner, W.B. (2005) The cell biology of neurogenesis. *Nat. Rev. Mol. Cell Biol.*, **6**, 777–788.
- Graus-Porta, D., Blaess, S., Senften, M., Littlewood-Evans, A., Damsky, C., Huang, Z., Orban, P., Klein, R., Schittny, J.C. and Müller, U. (2001) β 1-Class integrins regulate the development of laminae and folia in the cerebral and cerebellar cortex. *Neuron*, **31**, 367–379.
- Loulier, K., Lathia, J.D., Marthiens, V., Relucio, J., Mughal, M.R., Tang, S.C., Coksaygan, T., Hall, P.E., Chigurupati, S., Patton, B. *et al.* (2009) Beta1 integrin maintains integrity of the embryonic neocortical stem cell niche. *PLoS Biol.*, **7**, e1000176.
- Noctor, S.C., Flint, A.C., Weissman, T.A., Wong, W.S., Clinton, B.K. and Kriegstein, A.R. (2002) Dividing precursor cells of the embryonic cortical ventricular zone have morphological and molecular characteristics of radial glia. *J. Neurosci.*, **22**, 3161–3173.

29. Anthony, T.E., Klein, C., Fishell, G. and Heintz, N. (2004) Radial glia serve as neuronal progenitors in all regions of the central nervous system. *Neuron*, **41**, 881–890.
30. Spassky, N., Merkle, F.T., Flames, N., Tramontin, A.D., Garcia-Verdugo, J.M. and Alvarez-Buylla, A. (2005) Adult ependymal cells are postmitotic and are derived from radial glial cells during embryogenesis. *J. Neurosci.*, **25**, 10–18.
31. Klioueva, I.A., Van Luijtelar, E.L., Chepurnova, N.E. and Chepurnov, S.A. (2001) PTZ-induced seizures in rats: effects of age and strain. *Physiol. Behav.*, **72**, 421–426.
32. Santi, M.R. and Golden, J.A. (2001) Periventricular heterotopia may result from radial glial fiber disruption. *J. Neuropathol. Exp. Neurol.*, **60**, 856–862.
33. Schmechel, D.E. and Rakic, P. (1979) A Golgi study of radial glial cells in developing monkey telencephalon: morphogenesis and transformation into astrocytes. *Anat. Embryol. (Berl.)*, **156**, 115–152.
34. Miyata, T. and Ogawa, M. (2007) Twisting of neocortical progenitor cells underlies a spring-like mechanism for daughter-cell migration. *Curr. Biol.*, **17**, 146–151.
35. Takeichi, M. (2007) The cadherin superfamily in neuronal connections and interactions. *Nat. Rev. Neurosci.*, **8**, 11–20.
36. Alvarez-Buylla, A. and Lim, D.A. (2004) For the long run: maintaining germinal niches in the adult brain. *Neuron*, **41**, 683–686.
37. Lathia, J.D., Patton, B., Eckley, D.M., Magnus, T., Mughal, M.R., Sasaki, T., Caldwell, M.A., Rao, M.S., Mattson, M.P. and Ffrench-Constant, C. (2007) Patterns of laminins and integrins in the embryonic ventricular zone of the CNS. *J. Comp. Neurol.*, **505**, 630–643.
38. Kim, H., Nakamura, F., Lee, W., Hong, C., Pérez-Sala, D. and McCulloch, C.A. (2010) Regulation of cell adhesion to collagen via beta1 integrins is dependent on interactions of filamin A with vimentin and protein kinase C epsilon. *Exp. Cell Res.*, **316**, 1829–1844.
39. Ivaska, J., Vuoriluoto, K., Huovinen, T., Izawa, I., Inagaki, M. and Parker, P.J. (2005) PKCepsilon-mediated phosphorylation of vimentin controls integrin recycling and motility. *EMBO J.*, **24**, 3834–3845.
40. Kim, H., Nakamura, F., Lee, W., Shifrin, Y., Arora, P. and McCulloch, C.A. (2010) Filamin A is required for vimentin-mediated cell adhesion and spreading. *Am. J. Physiol. Cell Physiol.*, **298**, 221–236.
41. Fortin, S., Le Mercier, M., Camby, I., Spiegl-Kreinecker, S., Beger, W., Lefranc, F. and Kiss, R. (2010) Galectin-1 is implicated in the protein kinase C/vimentin-controlled trafficking of integrin-β1 in glioblastoma cells. *Brain Pathol.*, **20**, 39–49.
42. Leask, A., Shi-Wen, X., Khan, K., Chen, Y., Holmes, A., Eastwood, M., Denton, C.P., Black, C.M. and Abraham, D.J. (2008) Loss of protein kinase Cepsilon results in impaired cutaneous wound closure and myofibroblast function. *J. Cell Sci.*, **121**, 3459–3467.
43. Loo, D.T., Kanner, S.B. and Aruffo, A. (1998) Filamin binds to the cytoplasmic domain of the beta1-integrin identification of amino acids responsible for this interaction. *J. Biol. Chem.*, **273**, 23304–23312.
44. Noctor, S.C., Martinez-Cerdeno, V., Ivic, L. and Kriegstein, A.R. (2004) Cortical neurons arise in symmetric and asymmetric division zones and migrate through specific phases. *Nat. Neurosci.*, **7**, 136–144.
45. Noctor, S.C., Martinez-Cerdeno, V. and Kriegstein, A.R. (2008) Distinct behaviors of neural stem and progenitor cells underlie cortical neurogenesis. *J. Comp. Neurol.*, **508**, 28–44.
46. Lien, W.H., Klezovitch, O., Fernandez, T.E., Delrow, J. and Vasioukhin, V. (2006) AlphaE-catenin controls cerebral cortical size by regulating the hedgehog signaling pathway. *Science*, **311**, 1609–1612.
47. Woodhead, G.J., Mutch, C.A., Olson, E.C. and Chenn, A. (2006) Cell-autonomous beta-catenin signaling regulates cortical precursor proliferation. *J. Neurosci.*, **26**, 12620–12630.
48. Katayama, K., Melendez, J., Baumann, J.M., Leslie, J.R., Chauhan, B.K., Nemkul, N., Lang, R.A., Kuan, C.Y., Zheng, Y. and Yoshida, Y. (2011) Loss of RhoA in neural progenitor cells causes the disruption of adherens junctions and hyperproliferation. *Proc. Natl Acad. Sci. USA*, **108**, 7607–7612.
49. Lange, M., Winner, B., Müller, J.L., Marienhagen, J., Schröder, M., Aigner, L., Uyanik, G. and Winkler, J. (2004) Functional imaging in PNH caused by a new FilaminA mutation. *Neurology*, **62**, 151–152.
50. Scherer, C., Schuele, S., Minotti, L., Chabardes, S., Hoffmann, D. and Kahane, P. (2005) Intrinsic epileptogenicity of an isolated periventricular nodular heterotopia. *Neurology*, **65**, 495–496.
51. Tassi, L., Colombo, N., Cossu, M., Mai, R., Francione, S., Lo Russo, G., Galli, C., Bramerio, M., Battaglia, G., Garbelli, R. *et al.* (2005) Electroclinical, MRI and neuropathological study of 10 patients with nodular heterotopia, with surgical outcomes. *Brain*, **128**, 321–337.
52. Solé, G., Coupury, I., Rooryck, C., Guérineau, E., Martins, F., Devés, S., Hubert, C., Souakri, N., Boute, O., Marchal, C. *et al.* (2009) Bilateral periventricular nodular heterotopia in France: frequency of mutations in FLNA, phenotypic heterogeneity and spectrum of mutations. *J. Neurol. Neurosurg. Psychiatry*, **80**, 1394–1398.